IJESG
e-ISSN 2636-7904
International Journal of Energy and Smart Grid
Vol 9, Number 1, 2024
Doi: 10.55088/ijesg.1449194

Research Article

MODELLING AND EXERGETIC TECHNO-ECONOMIC ANALYSIS OF A SYSTEM FOR HYDROGEN PRODUCTION FROM EMPTY BANANA FRUIT BUNCH

Akpaduado Friday JOHN*[1], Joseph Oyekale OYETOLA[2]

[1]Department of Mechanical Engineering, Federal University of Petroleum Resources Effurun, PMB 1221 Effurun, Nigeria. Orcid[1]: https://orcid.org/ 0000-0002-8220-7093
[2]Department of Mechanical Engineering, Federal University of Petroleum Resources Effurun, PMB 1221 Effurun, Nigeria. https://orcid.org/ 0000-0003-4018-4660
* Corresponding author; afj223@lehigh.edu

Abstract: *One of the most effective and reliable methods for generating hydrogen fuel using biomass is the gasification method. However, using different biomass feedstock can withstand syngas production, which can be utilized for several applications. The study investigated the feasibility of hydrogen from Empty Banana Fruit Bunch (EBFB) biomass and the energetic techno-economic analyses of biomass gasification plants with a developed system simulation model, Aspen Plus simulator V11. Five chemical reactions were used in the production process and were simulated in ASPEN Plus simulator through biomass gasification method which aimed to remove C, CO, CO_2, CH_4, and H_2O to convert them into hydrogen gas. However, the total exergy-out divided by the total exergy-in gives exergy efficiency. Hence, total energy-out subtracted from total exergy-in depicts exergy destruction. The exergoeconomic method utilized in the exergoeconomic analyses is the Specific Cost method (SPECO). The results affirmed that 80.465 kg/h of H_2 can be produced from 2000 kg/h of empty banana fruit bunch at every 39.92 k mol/h mole flow of Empty Banana Fruit Bunch (EBFB). However, at a temperature below 900 degrees Celsius (^{o} C), CO decreases, and CO_2 increases. Above 1000 degrees Celsius (^{o} C), CO increases hence, decreasing CO_2 emission. The system total exergy in, total exergy out, percentage exergy efficiency, and exergy destruction are 4534.77 kJ/kg, 3857.295 kJ/kg, 0.8506 %, and 677.475 kJ/kg. Hence, system exergy stream cost rate, component-related cost rate, component-related cost difference, and component exergoeconomic factor are 407527.644 $/h, 1555.57 $/h, 0.5679 %, and 0.9089 % respectively. Further studies may concentrate on reducing CO through regulated temperature and pressure differences to increase the quantity of hydrogen production.*

Keywords: *Biomass; sensitivity analysis; empty banana fruit bunch; combustor; gasifier; separator; exergy; exergoeconomic*

Received: March 8, 2024 *Accepted: December 16, 2024*

1. Introduction

Hydrogen fuel has been recommended as an alternative to reduce the reliance on fossil fuels. Investigations confirmed that over 92.5 billion kilograms of hydrogen are being produced annually and that 76 % of hydrogen production globally is from reforming natural gas via steam methane reformer, 22 % from coal gasification (primarily from China), and only 2 % from water electrolysis, respectively [1-2]. It has been proven beyond a reasonable doubt that hydrogen fuel is a clean energy source that does not damage the environment and liberates only water as effluent when utilized in a fuel cell system. Hydrogen can however be obtained via various renewable energy raw materials [3-5]. Renewable energy sources like solar, hydro, wind, and biomass, along with domestic resources like nuclear power and natural gas. The above attributes and much more increase the importance of this fuel as a better and more reliable fuel, especially for industrial use, transportation, power generation, grid balancing, petrochemical, and refinery processing. Its usefulness can never be overemphasized, fueling cars, running generators in houses, for portable power, etc. Due to its nature, hydrogen can be used to move, store, and deliver energy produced from other sources [6]. Ping et al. analyzed the significant impact of

hydrogen on the economy in clean energy technologies [7]. Hence, a detailed description of a dehydrogenation route that applies to different non-food-related biomass waste. Most especially wheat straw, corn straw, rice straw, reed, bagasse, bamboo sawdust, and cardboard. His observation affirmed the possibility of H_2 yields up to 95 % from a one-pot, two-step reaction with a 69 ppm molecularly iridium catalyst, imidazoline moiety in formic acid, through a 1 v % dimethyl sulfoxide of biomass. Hydrogen does not exist alone. It is extracted from other elements in the molecule in which it occurs. Investigation proved that hydrogen exists in numerous sources hence, different methods of producing hydrogen [8]. Biomass is a renewable organic resource. This technology includes agriculture crop residues e.g., corn stove or wheat straw, forest residues, special crops grown specifically for energy consumption e.g., switch grass or willow trees, organic municipal solid waste, and animal wastes. Biomass produces hydrogen along with other by-products by gasification. Literature confirms that the combination of agricultural biomass, heat, steam, and oxygen at temperatures above 700 degrees Celsius, without combustion, liberates hydrogen [10-13]. This process is known as hydrogen production through biomass gasification (Figure 1).

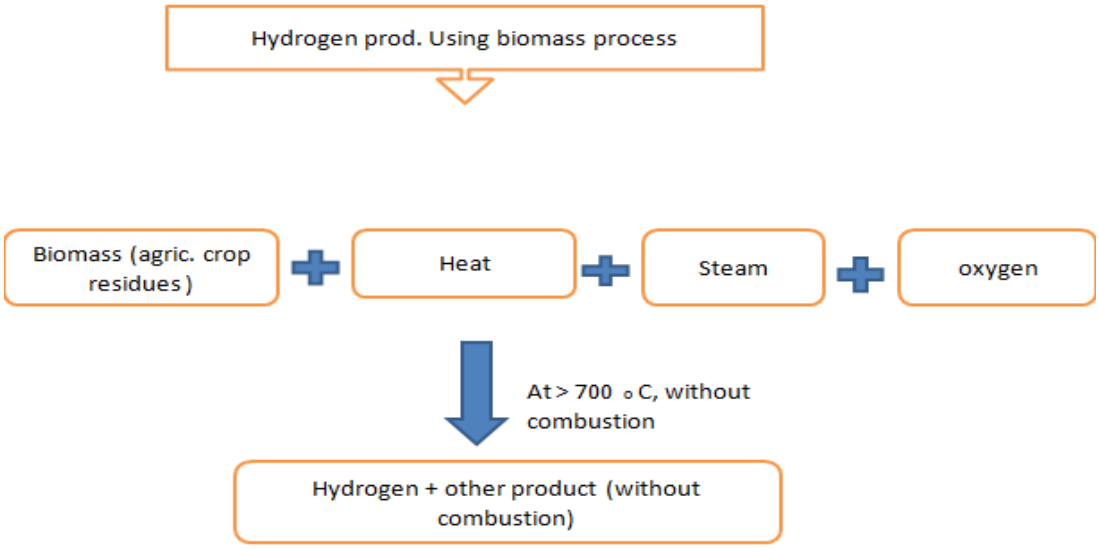

Figure 1. Hydrogen production through biomass gasification

Gasification is a key technology in hydrogen production, wherein biomass undergoes thermal decomposition in a low-oxygen environment rather than combustion. This process utilizes a controlled methodology to convert biomass into hydrogen and a variety of other gaseous by-products. By carefully managing temperature, pressure, and reactant flow, the gasification process optimizes the yield and purity of hydrogen, making it a viable option for sustainable energy solutions [14-15]. Chen et al. (2010) produced hydrogen using the biomass gasification method in supercritical water with the help of concentrated solar energy [9]. Agricultural residue like rice husks, cereal straws, coconut husks, maize cob, empty banana bunch, etc. is normally utilized for gasification through biomass. Others include charcoal, wood waste, peat, and wood. Marcantonio et al. (2019) considered biomass feedstock to generate syngas consisting of H_2, CO, and CH_4, which can also be utilized for several applications. Investigations have revealed that food waste valorization to hydrogen is a viable energy source with potential economic benefits [20-21]. The concept of exergy analysis elucidated and showcased causes for the inefficient performance of components. This concept allows accurate quality energy determination for the causes and reveals losses even when determining the residues in heat generation processes in a thermal plant. This deals with the performance of chemical processes. Exergy consists of

four elements: physical, chemical, kinetic, and potential energies. The combination of exergy analysis and economic principles, such as assisting in the verification of cost flow in a system and optimizing the system performance is termed exergoeconomic [22]. In upgraded exergoeconomic analysis, the specific capability of various industrial processes is utilized to find the exergy destruction hence, inversion cost rates to step up the sustainability of a plant. The exergoeconomic method adopted in the energy-economic analysis is the Specific Cost method (SPECO). Fuel and product of components are defined using direct capturing of a systematic value of all the stream exergy entering and subtracting from all the stream exergy leaving the component. The component-related cost difference and rate average cost per exergy unit production are calculated based on SPECO principles. Cabezas et al. (2020) affirmed that exergy efficiency gives more realistic specifications than the corresponding energy efficiency because exergy efficiency provides more understanding of performance. Results affirmed that exergy analysis methods of availability improve greater efficiency to define the second operational flow efficiency [8]. Xu et al. (2018) analyzed the exergy analysis of hydrogenation via gasification of steam through biomass as a renewable source. The steam biomass rate flow rate initially increases and finally decreases the efficiency due to exergy. Moreover, reaction catalysts may have positive, negative, or negligible efficiency issues due to exergy, whereas residence time generally has a slight efficiency issue due to the exergy [26-28]. Olusegun et al. (2023) investigated the generation of biodiesel from rubber seed oil by comparing the ethyl-based HCR and MSR. The Aspen Hysys engineering tool was utilized in the simulations to investigate the ethanolysis process for RSO in both HCRs and MSRs. The results affirmed that HCR can convert 99.01 % of RSO compared to the MSR's 94.85 % [25]. Chen et al. (2010) adopted a concentrated solar energy method with the help of superficial water in a gasification plant for hydrogen [9]. Arafat & Dincer, (2016) produced his hydrogen from oil palm biomass with the help of a water gas-shift gasification method [1]. Marcantonio et al. (2019) got their hydrogen from agricultural feedstock by adopting biomass gasification methods. Nevertheless, researchers have extensively addressed fossil fuel substitutes from both individual and institutional perspectives through their numerous works. Hence, despite their studies, the following main points are however pointed out as a base factor for Empty Banana Fruit Bunch (BEFB) consideration;

- Less attention has been given to Empty Banana Fruit Bunch (BEFB) for hydrogen production through a series of perceptions as to the levels of implementation of their research. During combustion, Empty Banana Fruit Bunch (BEFB) minimal carbon dioxide is emitted,
- Availability of Empty Banana Fruit Bunch (BEFB), less or no pollution of the immediate environment and the agricultural biomass is not in competition with human food,
- The use of renewable energy sources over fossil fuels reduces carbon emissions, promoting clean energy and protecting the ozone layer. Empty Banana Fruit Bunch (BEFB) can generate high energy efficiency due to its ability to emit low or no net CO2 during combustion [16-20].

To bridge this gap, this study aims to apply the Aspen Plus software to model and assess the feasibility of a system for hydrogen production from empty banana fruit bunch for electricity generation and to adopt a conventional exergy and exergoeconomic analyses calculator in solving thermal losses in the gasification power plant. The specific objectives are;

i. To model and simulate a hydrogen production system from an empty banana fruit bunch (EBFB) using Aspen plus simulator;
ii. To investigate the sensitivities of some system components such as gasifier, combustor, and separator to variations in thermodynamic properties such as temperature and pressure;
iii. To assess the operational technicality of the system hence, system components by utilization of a conventional exergy analysis approach;

iv. To assess the economic system performance using a classical energy-economic method.

Section two of the paper outlines the methodology used in this study. Results are presented and discussed in section three, and the main conclusions are summarized in section four.

2. Methodology

2.1. Simulation model

Assumption

The following depict assumptions were made in modeling the gasification process (Marcantonio et al., 2019), (Lim et al., 2018).

- Drying and pyrolysis did not occur instantaneously, and volatile products mainly consist of H_2, N_2, O_2, CO_2, CO, CH_4, and H_2O,
- The process is in steady-state and isothermal,
- No pressure drop and heat loss were considered during the simulation (all gases behave ideally). All considered components are in chemical equilibrium,
- Sulfur, nitrogen, and chlorine in the biomass flow into the gas phase of the process. The char/ash is a hundred percent carbon.

2.2. Process scheme

Figure 2 depicts the schematic of the gasification of biomass for the extraction of hydrogen in the study. The biomass feedstock adopted was Banana Empty Fruit Bunch (BEFB). The RSTOIC (drying) and the RYIELD stage simulate the first part of the gasification process and produce H_2, CH_4, H_2O, CO, CO_2, and ash.

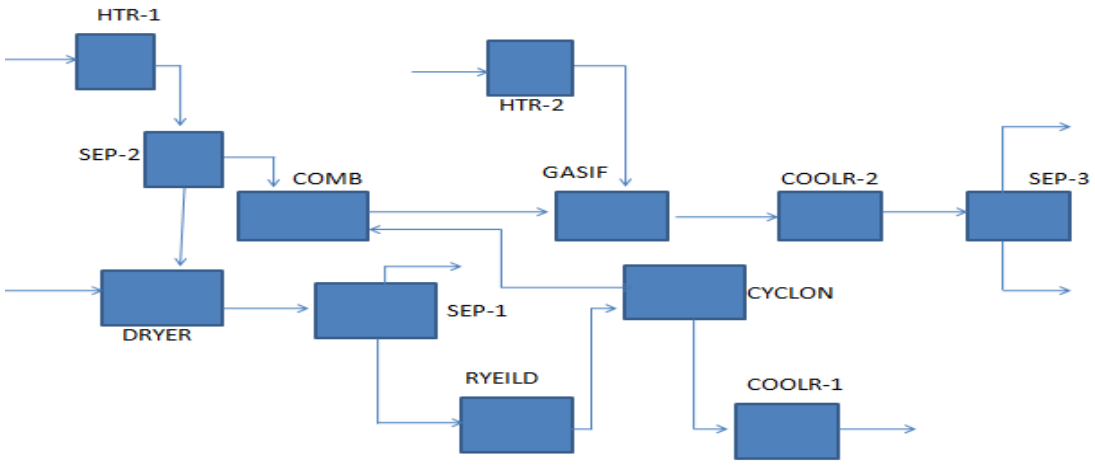

Figure 2. Schematic of biomass gasification of the hydrogen production process

Table 1. Aspen plus flow-sheet unit operations

Aspen plus name	Block ID	Function
RSTOIC	RSTOIC	Rstoic reactor (dryer) – simulates the biomass by drying the biomass before going into a separator (SEP-1).
SEP	SEP	Separator: SEP-1; separates the biomass into two streams before entering the Ryield reactor. N_2 + H_2O in a stream and dry biomass in another stream. SEP-2: separates the atmospheric air, delivers N_2 into the RSTOIC and O_2 into the COMBUSTOR. SEP-3; extracts pure hydrogen, and syngas with 75 % efficiency
HEATER	HEATER	Heater-1 increases atm air and delivers into SEP-2. Heater-2 increases atm air and delivers into the combustor.
R-YIELD	DECOMP	Yield reactor - converts the non-conventional stream dry-biomass from SEP-1 into its conventional components (C, H, O).
SSplit	CYCLONE	SSplit- removes ash from the pyrolysis before entering the COOLER-1 and delivers the conventional biomass into the COMBUSTOR.
COOLER	COOLER	Cooler-1 lowers the ash temperature; Cooler-2 lowers the gasifier product temperature.
RGIBB'S	COMBUSTOR GASIF	Combustor (Gibb's free energy reactor)-combines the conventional biomass from the SSplit with O_2 from SEP-2 at high temperature. Gibb's free energy reactor (simulates, partial oxidation, and gasification) at restricted chemical equilibrium of the specified reaction aligns the syngas composition in specifying a temperature approach for each reaction.

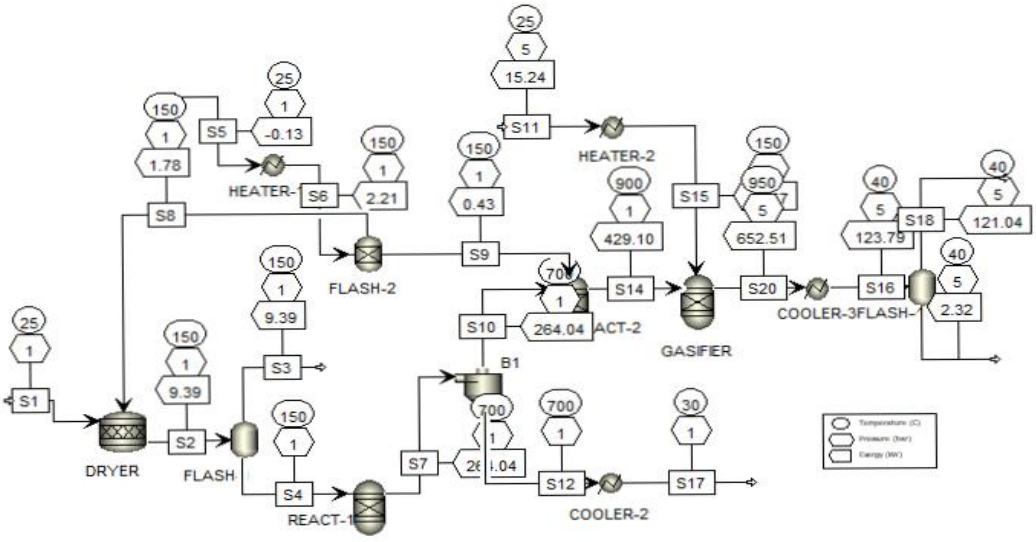

Figure 3. Investigated system components Flow-sheet

The simulation flow sheet developed through a sequence of stages with Aspen Plus is depicted in Figure 3. Table 1 depicts each unit of operational processes in the gasification plant. The atmospheric air at 25 degrees Celsius (°C) temperature and pressure of 1 bar flow at 400 kgh-1 flow rate into the heater block (HEATER-1), the heater increases the temperature to about 150 degrees Celsius (°C) at a constant pressure of 2 bar. Increase holding pressure constant at atmospheric temperature, heater-1 delivers the hot air containing nitrogen and oxygen gases into the separator (FLASH-2). At a Steady

flow rate of 2000 kghr-1, the biomass stream, constituted of Banana Empty Fruit Bunch (BEFB), goes into the Rstoic block (RSTOIC reactor) at 150 degrees Celsius (°C) and 1 bar. The RSTOIC reactor stimulates the biomass by drying (with nitrogen, N_2 from SEP-1) into dry biomass before entering into the separator-1 (SEP-1). The dry biomass from the stock is at 150 degrees Celsius (°C) and 1 bar enters the separator (FLASH). The separator of the same pressure and temperature splits the stream from the dryer into two streams. The first stream (stream 3) contains (N_2 + H_2O) nitrogen gas and the remaining quantity of water from the dry biomass because water is not completely removed from the dryer (stock). The second stream (stream 4) at the same pressure and temperature containing the dry biomass enters the DECOMP block (RYIELD reactor). The yield reactor, at 700 degrees Celsius (°C) and 1.5 bar converts the non-convectional dry biomass into conventional components (pyrolysis). The cyclone is an ash removal block. It removes all available ash from the pyrolysis (YIELD reactor) and delivers ash through the ash removal stream into a cooler-1 (Requil reactor) at the same temperature and pressure. The cooler-2 block drastically reduces the temperature to 400 degrees Celsius (°C) and pressure of 5 bar. Hence, the conventional elements (C, H, O), from the cyclone enter the combustor block at 900 degrees Celsius (°C) and 4 bar. Oxygen gas O_2 from the separator (FLASH -2) at 150 degrees Celsius (°C) and 1 bar for convectional elements from the cyclone in the combustor (COMB block). Combustor products at 900 degrees Celsius (°C) and 4 bar enter the gasifier (Gibb's free reactor). The dry-biomass conventional elements (C, H, O) are heated at a temperature above 700 degrees Celsius (°C) say degrees Celsius (°C) at 4 bars without combustion, and combustion products are made to enter into the Gibb's free reactor (gasifier). At 150 degrees Celsius (°C) and 2 bar, oxygen O_2 gas from atmospheric air from HEATER-2 into the gasifier for gasification. The heater-2 increases the atmospheric air to liberate O_2 at 150 degrees Celsius (°C) and 2 bar and delivers O_2 into the gasifier for the gasification process at 950 degrees Celsius (°C) and 5 bar. Proper process simulation occurs in Gibb's reactor for individual reactions at 950 degrees Celsius (°C) and 5 bar. This temperature is preferable in the simulation process because at temperatures higher than 1000 degrees Celsius (°C), there is an increase in the amount of carbon monoxide, and CO produced and a decrease in the amount of CO_2 produced. On the other hand, at a temperature below 900 degrees Celsius (°C), a higher amount of CO_2 is produced, hence, lessening the amount of CO_2, and CO produced (Zhenling et al., 2017). The gasifier product is discharged from the gasifier at 950 degrees Celsius (°C) and 5 bar then enters a cooler (COOLER-3). At constant pressure, the cooler reduces the temperature to about 40 degrees Celsius (°C) and 5 bar before entering a separator (SEP-3). This is done to reduce the temperature as a higher temperature can damage the separator or reduces the separator's efficiency. At the separation unit, a SEP ID block (FLASH-3) unit is required to gain high hydrogen purity at 40 degrees Celsius (°C) and 5 bar. Moreover, the characteristics and features of the apparatus used in the simulation were determined from the optimized values found in the literature for these membranes. The separator (FLASH -3) at 40 degrees Celsius (°C) and 5 bar split the gasifier product into two streams (stream 18 & stream 19). Stream 18 depicts the percentage of hydrogen H_2 and a minor fraction of other gases produced. The other stream (stream 19) reviews the amount of CO_2, CO, H_2O, and other gas released. The equilibrium reactions are restricted five consecutive equations are formed in combustion and gasifier Tables 4 & 5 [23, 24 & 28].

Physical and chemical properties of EBFB

Five chemical reactions were employed in combustion and gasification processes to produce highly purified hydrogen gas. Table 2 presents the ultimate and proximate analysis of simulated data for banana empty fruit bunch (BEFB) from kinds of literature (Sugumaram et al., 2012), (Marcantonio et al., 2019). These reactions were simulated using ASPEN Plus, to remove carbon (C), carbon monoxide (CO), carbon dioxide (CO_2), methane (CH_4), and water (H_2O) to convert them into hydrogen gas. The

combustion process consists of three chemical reactions, while the gasification process includes two reactions.

Table 2. General physical and chemical properties of empty banana fruit bunch **(**EBFB**)**

Properties	**Biomass value** **Empty fruit bunch (EFB)**
Ultimate analysis	
Carbon (%)	41.75
Oxygen (%)	51.73
Hydrogen (%)	5.10
Nitrogen (%)	1.23
Sulfur (%)	0.18
Proximate analysis	
Fixed carbon (%)	5.95
Moisture content (%)	5.21
Volatile matter (%)	78.83
Ash	15.73
Sulfanal analysis	
Organic % dry mass	0.18
Pyritic % dry mass	0
Sulfate % dry mass	0

Combustor

The three reactions considered in combustion with their stoichiometry reaction are listed in Table 3. Boundary condition was set in ASPEN Plus to carry out the reactions with the equations restricted to the chemical equilibrium specified temperature approach. The combustor operational condition was 900 degrees Celsius (^{o}C) and 4 bar. Nitrogen gas from SEP-2 (FLASH-2) at 200 kg hr-1 flow rate, 150 degrees Celsius (^{o}C), and 2 bar in the combustion process. The number of iterations considered is 30 with 0.0001 error tolerance.

Table 3. Combustion reactions

Specification Type	**Stoichiometry**	**Reaction name**
Temp. approach	$C + ½O_2 \Rightarrow CO$	Ash partial combustion
Temp. approach	$H2 + ½O_2 \Rightarrow H_2O$	H_2 partial combustion
Temp. approach	$CO + ½O_2 \Rightarrow CO_2$	CO shift

Gasifier

Two reactions considered in the gasification process are listed in Table 4**.** Oxygen gas O_2 from atmospheric air at 200 kg hr -1 flow rate, 150 degrees Celsius (^{o}C), and 1.1 bar in Gibb's reactor. The maximum accuracy is 30 with 0.0001 error tolerance. The temperature at 950 degrees Celsius (^{o}C) and pressure of 5 bar were set as a gasifier boundary condition. Oxygen from atmospheric air at 150 degrees Celsius (^{o}C) gas O_2 for process gasification 200 kg hr-1 flow rate. The composition of the stream exits the gasifier into the separator (HEATER-2).

Table 4. Gasifier reactions

Specification Type	Stoichiometry	Reaction name
Temp. approach	$C + H_2O \Rightarrow CO + H_2$	Water gas
Temp. approach	$CO + H_2O \Rightarrow CO + H_2$	CO shift

Separation units

SEP-1; The separator (FLASH-1) at 150 degrees Celsius (° C) and 2 bar separates the nonconventional biomass from the Rstoic into two streams: N_2 and H_2O into streams (stream 3) hence, dry-biomass into the second stream (stream 4) before entering into RYIELD reactor where the nonconventional dry biomass is broken down into smaller conventional unit (C, H, O).

SEP-2; A PSA unit at 150 degrees Celsius (° C) and 2 bar is required at an elevated temperature to gain high-purity delivery of N_2 and O_2. High-temperature atmospheric air from heater-1 is separated into nitrogen gas and oxygen gas through a separator (FLASH-2). The separator delivers nitrogen gas to the dryer (Rstoic) used for drying the biomass and delivers corresponding oxygen gas into Gibb's reactor for combustion.

SEP-3; The corresponding temperature and pressure values of SEP-3 utilized in the process concerning the efficiency were determined from the optimized values found in the literature. At 40 degrees Celsius (° C) and 5 bar, the separator separates the gasifier product from cooler-2 into two streams. In one stream carbon C and water H_2O in the other stream and a small fraction of CH_4, CO, CO_2, H_2O.

2.3. Sensitivity analysis

Components such as combustor, gasifier, and separator variation to present gases are examined through sensitivity analysis. This was performed with the Model Analysis Tools (MAT) in the Aspen Plus simulator. This is based on present gases in the components with 100 - 1000 manipulated variable limits starting and ending point limits and 50 division numbers of points. The Model Analysis Tools factor used for the block variable is 1.048113. The present gases for the sensitive modeling in the combustor block are: H_2, O_2, C, N_2, and S. For gasifier and separator (SEP-3) blocks, gases present are: H_2, O_2, N_2, H_2O, CO, CO_2, CH_4, NH_3, H_2S.

2.4. Concept of exergy

In the absence of the nuclear effect, magnetism, electricity, and surface tension exergy of a stream are segmented into distinct components: physical exergy, chemical exergy, kinetic exergy, and potential exergy (T.J. Kotas 1995, Exergy concepts).

Mathematically,

$$É = Ék + Ép + Éph + Ech \quad (1)$$

From where $\boldsymbol{\varepsilon k}$ is the kinetic exergy, $\boldsymbol{\varepsilon p}$ potential exergy, Eph exergy due to physical, and $\boldsymbol{\varepsilon ch}$ is the chemical exergy. Because the kinetic and potential exergies are accomplished under low and high-grade energy, they are usually negligible during calculation.

If ε equals the specific exergy of the system, then introducing the specific exergy from where

$$\boldsymbol{\varepsilon} = É/m \quad (2)$$

Hence,

$$\boldsymbol{\varepsilon} = \boldsymbol{\varepsilon k} + \boldsymbol{\varepsilon p} + \boldsymbol{\varepsilon ph} + \boldsymbol{\varepsilon ch} \quad (3)$$

Physical exergy of a perfect gas

This exergy is equal to the maximum amount of work obtainable when the stream of substance when brought from its initial state to the environmental state defined by environmental pressure $P_0$and environmental temperature T_0, by physical processes involving only thermal interaction with the environment is termed the physical exergy of the system. The physical exergy of perfect gas can be calculated using the expression below:

$$\mathcal{E}Ph = (h - h0) - T0\,(S - S0) \quad (4)$$

Putting enthalpy and entropy equations into the physical exergy equation, we have physical exergy expression given that the surrounding temperature equals 298.15 K and 1 atm,

However, the general formula for physical exergy is given by;

$$\mathcal{E}Ph = CP(T1 - T0 - T0\,InT1/T0) + RT0\,In\,(P1/P0) \quad (5)$$

Therefore, writing the general physical exergy equation concerning each block in the gasification power plant flow sheet with constant surrounding temperature T_0 and pressure P_0 (in 273.150K and 1bar), specific heat capacity C_P, and molar gas constant R (mean of C_P and R gases present per component, supplementary table 7 & supplementary table 8).

For DRYER: $\mathcal{E}PhDRYR$, SEP-1: $\mathcal{E}PhSEP - 1$, RYEILD: $\mathcal{E}PhRYD$, CYCLONE: $\mathcal{E}PhCYLN$, HEARTER-1:$\mathcal{E}PhHTR - 1$, SEP-2: $\mathcal{E}PhSEP - 2$, COOL-1: $\mathcal{E}PhCOOL - 1$, COMBUSTOR: $\mathcal{E}PhCOMB$, GASIFIER: $\mathcal{E}PhGASIF$, COOL-2: $\mathcal{E}PhCOOL - 2$, SEP-3: $\mathcal{E}PhSEP - 3$.

Standard molar chemical exergy for gas mixtures

A general formula for chemical exergy can be expressed as follows:

$$e\chi Ch - K = \sum i(\chi i * e\chi Ch) + RT0 \sum i(\chi i In\chi i) \quad (6)$$

where,

$$\sum i\chi i e\chi Ch = [(mole\ fraction\ of\ O2) * (standard\ chemical\ exergy\ of\ O2) + (mole\ fraction\ of\ CO2) * (standard\ chemical\ exergy\ of\ CO2) + (mole\ fraction\ of\ N2) * (standard\ chemical\ exergy\ of\ N2) + (mole\ fraction\ of\ H2O) * (standard\ chemical\ exergy\ of\ H2O)]$$

Hence,

$$e\chi Ch(i) = RT0In\,(P0/P(i)) \quad (7)$$

The partial pressure Pi and molar fraction of each substance air at a given relative humidity by Szargut et al. (1988). Mole fraction of combustion gases (Ibrahim Dincer and Marc. A. Rosen (Eds.) – Exergy, standard chemical exergy values for selected substances for air constituents adopted in the calculation of chemical exergies of various substances (boundary condition; T_0 = 298.15 K and P_0 = 1 atm), Kotas (1995), Bejan et al. (1996).

Assuming all gases behave ideally, the molar chemical exergy can then be fathomed using the below expression:

$$e\chi Ch - K = -RT0\,In(\chi iekP0\ /\ P0\ ) = -RT0\,In(\chi iek) \quad (8)$$

Thus, we need to write the general molar chemical exergy equation for the mixture of gases for each block in the biomass gasification power plant flow sheet.

DRYER: completely biomass, no chemical exergy formed: $e\chi Ch - K(DRYR)$ = Null

SEP-1: Constituent gases present are N_2 and H_2O: Standard molar chemical exergy with respect to SEP-1 equals:

$$e\chi Ch - K(SEP - 1) = \{(\chi N2 * e\chi ChN2) + (\chi H2O * e\chi ChH2O)\} + RT0\,\{(\chi N2 * In\chi N2) + (\chi H2O * In\chi H2O)\} \quad (9)$$

Where, $(e\chi Ch)N2, H2O = RT0In\,(P0/Pi, N2, H2O)$ (10)

RYEILD: Standard molar chemical exergy from the Ryeild reactor is null, as there are no constituent gases present

CYCLONE: H_2, O_2, N_2, C, and S - Therefore, standard molar chemical exergy due to cyclone

$$e\chi Ch - K(CYCL) = \{(\chi H2 * e\chi ChH2) + (\chi O2 * e\chi ChO2) + (\chi N2 * e\chi ChN2) + (\chi C * e\chi ChC) + (\chi S * e\chi Ch\,S)\} + RT0\,\{(\chi H2 * In\chi H2) + (\chi O2 * In\chi O2) + (\chi N2 * In\chi N2) + (\chi C * In\chi C) + (\chi S * In\chi S)\} \quad (11)$$

HEATER-1: Constituent gases present are O_2 and N_2:

$$e\chi Ch - K\,(HTR-1) = \{(\chi O2 * e\chi Ch\,O2) + (\chi N2 * e\chi ChN2)\} + RT0\,\{(\chi O2 * In\chi O2) + (\chi N2 * In\chi N2)\} \quad (12)$$

SEP-2: Constituent gases present are O_2 and N_2:

$$e\chi Ch - K\,(HTR-1) = (\chi O2 * e\chi Ch\,O2) + (\chi N2 * e\chi ChN2)\} + RT0\,\{(\chi O2 * In\chi O2) + (\chi N2 * In\chi N2)\} \quad (13)$$

COOLER -1: No constituent gas present. Therefore, $e\chi Ch - K\,(COOL-1) =$ null

COMBUSTOR: Constituent gases present are H_2, O_2, N_2, C, and S: Standard molar chemical exergy due combustor;

$$e\chi Ch - K\,(COMB) = \{(\chi H2 * e\chi Ch\,H2) + (\chi O2 * e\chi ChO2) + (\chi N2 * e\chi Ch\,N2) + (\chi C * e\chi Ch\,C) + (\chi S * e\chi Ch\,S)\} + RT0\,\{(\chi H2 * In\chi H2) + (\chi O2 * In\chi O2) + (\chi N2 * In\chi N2) + (\chi C * In\chi C) + (\chi S * In\chi S)\} \quad (14)$$

GASIFIER: Constituent gases present are H_2, O_2, N_2, H_2O, CO, CO_2, CH_4, NH_3, and H_2S :Standard molar chemical exergy due gasifier;

$$e\chi Ch - K\,(GASIF) = \{(\chi H2 * e\chi Ch\,H2) + (\chi O2 * e\chi ChO2) + (\chi N2 * e\chi Ch\,N2) + (\chi H2O * e\chi Ch\,H2O)\,(\chi CO * e\chi Ch\,CO) + (\chi CO2 * e\chi Ch\,CO2) + (\chi CH4 * e\chi Ch\,CH4) + (\chi NH3 * e\chi ChNH3) + (\chi H2S * e\chi Ch\,H2S)\} + RT0\,\{(\chi H2 * In\chi H2) + (\chi O2 * In\chi O2) + (\chi N2 * In\chi N2) + (\chi H2O * In\chi H2O) + (\chi SCO * In\chi CO) + (\chi CO2 * In\chi CO2) + (\chi CH4 * In\chi CH4) + (\chi NH3 * In\chi NH3) + (\chi H2S * In\chi H2S)\} \quad (15)$$

HEATER- 2: Constituent gases present are O_2 and N_2: Standard molar chemical exergy with respect to heater- 2 reactor;

$$e\chi Ch - K\,(HTR-2) = \{(\chi O2 * e\chi Ch\,O2) + (\chi N2 * e\chi ChN2)\} + RT0\,\{(\chi O2 * In\chi O2) + (\chi N2 * In\chi N2)\} \quad (16)$$

COOLER-2: Constituent gases present are H_2, O_2, N_2, H_2O, CO, CO_2, CH_4, NH_3, and H_2S:

$$e\chi Ch - K\,(COOL-2) = \{(\chi H2 * e\chi Ch\,H2) + (\chi O2 * e\chi ChO2) + (\chi N2 * e\chi Ch\,N2) + (\chi H2O * e\chi Ch\,H2O)\,(\chi CO * e\chi Ch\,CO) + (\chi CO2 * e\chi Ch\,CO2) + (\chi CH4 * e\chi Ch\,CH4) + (\chi NH3 * e\chi ChNH3) + (\chi H2S * e\chi Ch\,H2S)\} + RT0\,\{(\chi H2 * In\chi H2) + (\chi O2 * In\chi O2) + (\chi N2 * In\chi N2) + (\chi H2O * In\chi H2O) + (\chi SCO * In\chi CO) + (\chi CO2 * In\chi CO2) + (\chi CH4 * In\chi CH4) + (\chi NH3 * In\chi NH3) + (\chi H2S * In\chi H2S)\} \quad (17)$$

SEP- 3: Constituent gases present are H_2, O_2, N_2, H_2O, CO, CO_2, CH_4, NH_3, and H_2S :

$$e\chi Ch - K\,(SEP-3) = \{(\chi H2 * e\chi Ch\,H2) + (\chi O2 * e\chi ChO2) + (\chi N2 * e\chi Ch\,N2) + (\chi H2O * e\chi Ch\,H2O)\,(\chi CO * e\chi Ch\,CO) + (\chi CO2 * e\chi Ch\,CO2) + (\chi CH4 * e\chi Ch\,CH4) + (\chi NH3 * e\chi ChNH3) + (\chi H2S * e\chi Ch\,H2S)\} + RT0\,\{(\chi H2 * In\chi H2) + (\chi O2 * In\chi O2) + (\chi N2 * In\chi N2) + (\chi H2O * In\chi H2O) + (\chi SCO * In\chi CO) + (\chi CO2 * In\chi CO2) + (\chi CH4 * In\chi CH4) + (\chi NH3 * In\chi NH3) + (\chi H2S * In\chi H2S)\} \quad (18)$$

Percentage exergy efficiency

Total exergy in of a system to the total exergy out of the same system defines the percentage exergy efficiency of that particular system. Hence, the total exergy is the sum total of exergies of all streams that enter the system. The total of exergies of all streams that flow out of the system refers to the total exergy out of a system.

$\%\ exergy\ eff\ =\ (Total\ exergy\ Out)\ /\ (Total\ exergy\ In)$

That is, $\eta ex\ =\ \sum Exergy\ Out\ /\ \sum Exergy\ In$ (19)

Exergy destruction analysis

The difference between the total exergy in and the total exergy out of a system dictates the exergy destruction of the system. Hence, exergy destruction is expressed mathematically as:

$Exergy\ destruction\ =\ Total\ exergy\ In\ -\ Total\ exergy\ Out$

$\dot{E}DESTRUCTION\ =\ \sum Exergy\ In\ -\sum Exergy\ Out$ (20)

2.5. Exergoeconomic analysis

The exergoeconomic method utilized in the energy-economic analysis is the Specific Cost method (SPECO). Fuel and products of components are defined by directly capturing the systematic value of all the stream exergy entering and subtracting the stream exergy leaving the component.

2.6. Component exergoeconomic factor analysis

Evaluating component performance, we are interested in the relative significance in terms of the cost-efficiency profitability of the entire system at a given period for each category in the gasification through biomass power plant. However, this is provided by the energy-economic factor f_K defined for component K as follows:

$fK\ =\ \dot{Z}K\ /(\dot{Z}K\ +\ Cf,k\ *\ (\dot{E}D,K)$ (21)

$\dot{Z}K\ =\ \dot{Z}K\ Cl\ +\ \dot{Z}K\ OM$ (22)

$\dot{Z}K\ Cl\ =\ CFR\ (i,n)\ *\ TCI$ OR $\dot{Z}K\ Cl\ =\ (CFR\ /top)\ *\ PEC$ (23a&b)

$\dot{Z}K\ OM\ =\ FOM*\ TCI$ OR $\dot{Z}K\ OM\ =\ \dot{Z}Cl*\ \varphi$ (24a&b)

Hence, $TCI\ =\ \varphi\ =\ PEC$

$CFR\ =\ \{i(1+i)\ n\}/\ (1+i)\ n-1$ (25)

However, the cost rate associated with capital, ŻK OM = operating maintenance expenses, ŻK = summation of ŻK OM and ŻK Cl, CFR (i,n) = cost rated with capital in respect to interest rate 'i' and payment period 'n', TCI = total cost investment, FOM = maintain cost factor, PEC = purchase investment cost, φ = factor of operating and maintaining expenses, top = time of operation, $\dot{E}D_K$ = exergy destruction with to the component under consideration and f_K= exergoeconomic factor. For this study, FOM = 1.06 for each piece of equipment, i = 6 %, top = 1hr, n = 25years, maintenance cost factor FOM, interest rate 'i' and the average cost 'Cf, k' values based on U.S. Department of Energy Federal Management Program, 15 Sept 2016, i = 0.06, n = 25yrs, FOM = 1.06, top = 1hr, Cf, k = $0.8(U.S. Department of Energy Federal Management Program (FEMP), 15 Sept 2016), (ATMACA et al., 2018). Note that the assumption was made on the total cost investment of the gasification of biomass components from Google.com as of 2022/23.

3. Result and Discussion

3.1. Modeling of a system for hydrogen production from the empty banana fruit bunch

Syngas, hydrogen production from empty banana fruit bunch (EBFB)

The separator (SEP-3) containing Stream 18 and Stream 19 revealed the syngas quantity produced from EBFB. The amount of syngas produced in stream 19 is presented in **Table 5**. Results affirmed that 80.465kg/h of hydrogen gas can be generated by 2000 kg/h of empty banana fruit bunch at every 39.916 km/h mole flows (Stream 18). It is also noted that the total volume of purified syngas generated during the gasification is 571.894 cum/h from stream 18, separator outlet. Hence, the total volume of lost syngas generated in stream 19, separator outlet is 0.118 cum/h volume of hydrogen gas. The gasification process of empty banana fruit bunches produces a significant amount of carbon monoxide, specifically 1,522.69 kg/h. The quality of this carbon monoxide has a direct impact on hydrogen gas production. In other words, as the quantity of carbon monoxide increases, the amount of hydrogen gas produced decreases. Hence, the relationship is influenced by the high temperatures in both the combustor and gasifier components.

Table 5. Stream 18 and 19 (S_{18} & S_{19}) separator outlet of syngas composition from Aspen Plus

	Units	S18	S19
Mass Flows	**kg/hr**	**2055.96**	**114.746**
H2	kg/hr	80.465	0.00161246
O2	kg/hr	5.16925e-05	1.64433e-08
N2	kg/hr	330.058	0.0858868
H2O	kg/hr	29.1057	113.908
CO	kg/hr	1522.64	0.424152
CO2	kg/hr	90.0953	0.290451
C	kg/hr	0	0
BIOMASS	kg/hr	0	0
ASH	kg/hr	0	0
CH4	kg/hr	0.000163313	1.07621e-07
NH3	kg/hr	0.00925685	0.000172678
S	kg/hr	0	0
H2S	kg/hr	3.5907	0.036269

	Units	S18	S19
Mass Fractions			
H2		0.0391374	1.40524e-05
O2		2.51427e-08	1.43301e-10
N2		0.160537	0.000748493
H2O		0.0141567	0.992692
CO		0.740597	0.00369643
CO2		0.0438214	0.00253125
C		0	0
BIOMASS		0	0
ASH		0	0
CH4		7.94336e-08	9.37906e-10
NH3		4.50244e-06	1.50487e-06
S		0	0
H2S		0.00174648	0.000316081
Volume Flow	cum/sec	0.158859	3.26705e-05

	Units	S18	S19
Mole Flows	**kmol/hr**	**109.826**	**6.34952**
H2	kmol/hr	39.9156	0.000799878
O2	kmol/hr	1.61545e-06	5.13872e-10
N2	kmol/hr	11.7821	0.00306591
H2O	kmol/hr	1.61561	6.32283
CO	kmol/hr	54.3598	0.0151426
CO2	kmol/hr	2.04716	0.00659969
C	kmol/hr	0	0
CH4	kmol/hr	1.01798e-05	6.7084e-09
NH3	kmol/hr	0.000543544	1.01393e-05
S	kmol/hr	0	0
H2S	kmol/hr	0.105355	0.00106417

	Units	S18	S19
Mole Fractions			
H2		0.363443	0.000125975
O2		1.47092e-08	8.09309e-11
N2		0.10728	0.000482857
H2O		0.0147106	0.995798
CO		0.494962	0.00238485
CO2		0.01864	0.0010394
C		0	0
CH4		9.26904e-08	1.05652e-09
NH3		4.94913e-06	1.59686e-06
S		0	0
H2S		0.000959289	0.000167599

3.2. Sensitivity analysis results

Effect of temperature and pressure on gasification (combustor, gasifier, and separator units)

A sensitivity analysis was performed for the combustor, gasifier, and separator (SEP-3) as regards temperature and pressure. Figure 4 affirmed that in the combustor, all the present gases (H_2, O_2, N_2, C, S) increase in a sinusoidal form except sulfur which exists as a solid at room temperature. However, for the gasifier, Figure 5 shows that the rate at which H_2, CO_2, NH_3, and CH_4 flow decreases drastically

hence, the rate at which O_2, N_2, CO, and H_2O flow produced inside the gasifier increases. However, the corresponding H_2S maintains a linear path between 3.60 kg/h and 3.65 kg/h. Figure 6 (SEP-3) shows that the rate at which H_2 is produced and flows increases from 3.525 kg/h to 3.62 kg/h and maintains a linear path. Hence, H_2O 3.64 kg/h decreases and maintains a linear path at 3.52 kg/h. Whereas, O_2 and CH_4 keep a constant linear path. Results show that corresponding effects occur in syngas concerning an increase in pressure. This implies that, at every instant of increase in temperature and pressure, there is a significant change in the flow rate of some gases at a certain kg/h in the combustor and gasifier and in the separator.

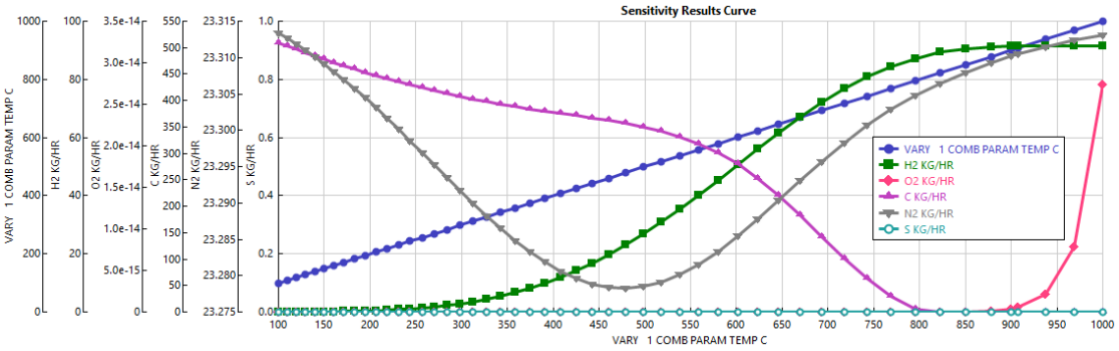

Figure 4. Gasification temperature effect on syngas out of combustor

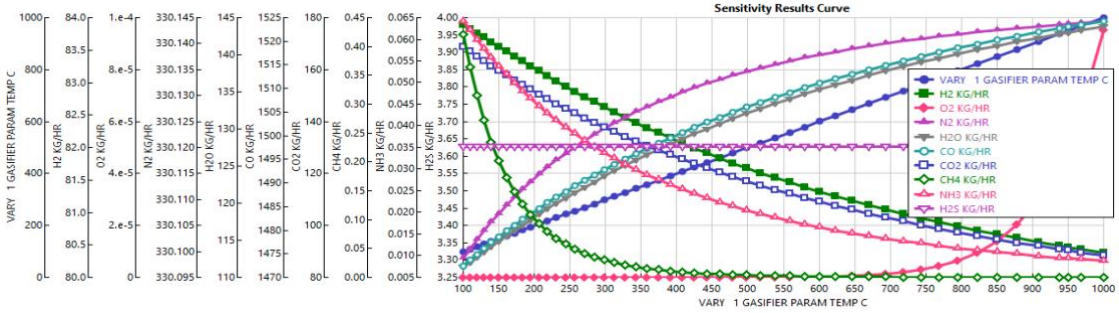

Figure 5. Gasification temperature effect on syngas out of gasifier

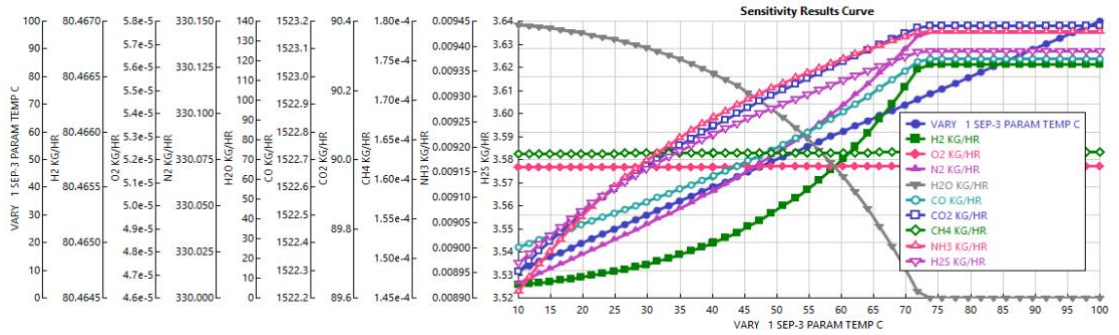

Figure 6. Gasification temperature effect on syngas out of the separator

3.3. Biomass gasification exergy results

Table 6 shows the system total exergy in, total exergy out, overall percentage exergy efficiency and exergy destruction are 4534.77 kJ /kg, 3857.295 kJ/kg, 0.8506 %, and 677.475 kJ/kg respectively. This indicates that a significant amount of energy is released during the gasification process, thereby

enhancing the sustainability of the biomass gasification system. However, high exergy destruction implies a loss of work in the system. Hence, the real processes are irreversible which measures the system degradation. Table 7 shows the components physical and chemical exergy of the system. The system's physical and chemical exergy is 36960.31 KJ/kg, 185.64 kJ/mol.

Table 6. Streams exergy, exergy efficiency, and exergy destruction table

COMPONENT	S. EXGY IN	S. EXGY OUT	% Ex eff (η)	$\dot{E}_{DESTRUCTION}$
DRYER	S_1, S_8 = 81.67	S_2 = 80.41	0.985	1.256
HEATER- 1	S_5 = 31.34	S_6 = 28.11	0.897	3.237
SEP- 1	S_2 = 180.41	S_3, S_4 = 155.22	0.860	25.198
SEP- 2	S_6 = 128.11	S_8, S_9 = 153.61	0.817	34.497
RYEILD	S_4 = 0	S7 = 563.55	0.00	0.00
CYCLONE	S_7 = 617,12	S_{10}, S_{12} = 609.12	0.987	0.800
COMBUSTOR	S_{10}, S_9 = 881.06	S_{14} = 872.40	0.990	8.656
GASIFIER	S_{14}, S_{15} = 1090.44	S_{20} = 1082.15	0.992	8.290
COOLER- 1	S_{12} = 0	S_{17} = 0	0.00	0.00
HEATER- 2	S_{11} = 137,16	S_{15} = 28.035	0.204	109.123
COOLER-2	S_{20} = 1082.15	S_{16} = 205.30	0.189	876.848
SEP- 3	S_{16} = 305.31	S_{18}, S_{19} = 284.69	0.932	20.612

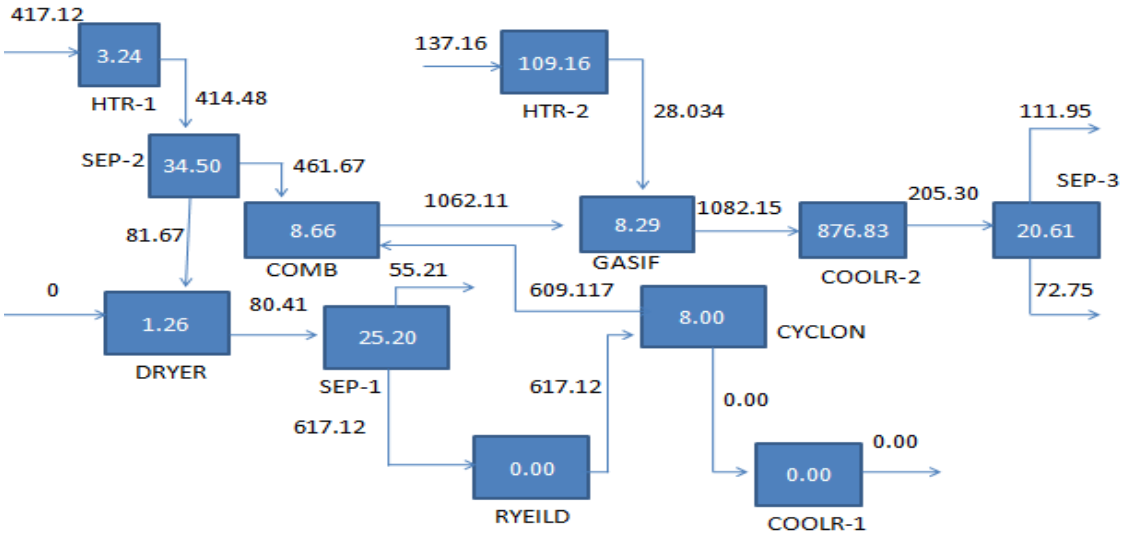

Figure 7. Block diagram for exergy flow in the biomass gasification plant (kW)

Figure 7 illustrates the gasification exergy process flow within the system. Exergy destruction of each component, subtracted from the total exergy of all incoming streams, must be equal to the total exergy of all outgoing streams from that component. Therefore, the block exergy flow diagram for the gasification of the biomass system is balanced.

3.4. Exergoeconomic analysis results

Table 7 and Table 8 present the Block physical and chemical exergy, rate due investment, and exergoeconomic evaluation results. The system exergy stream cost rate, component-related cost rate,

component-related cost difference, component exergoeconomic factor, and cost rate exergy destruction concerning fuel exergy destruction, cost rate exergy destruction concerning fixed product exergy destruction are 407527.644 $/h, 1555.57 $/h, 0.5679 %, 0.9089 %, 353.22 $/h, 73.135 $/h. The results from the evaluation show the necessity to improve the exergy utilization in some components such as cyclone, combustor, gasifier cooler-2, and SEP-3.

Table 7. Block physical and chemical exergy, rate due investment, and exergoeconomic factor results

COMPONENT	$\mathcal{E}_{Ph}$ (KJ/kg)	$e\chi_{Ch}^{-K}$(KJ/mol)	$\dot{Z}_{K,\,nth}$	f_K (%)
DRYER	80.84	0	2162.62	0.9993
HEATER- 1	78.47	19.36	1138.22	0.3862
SEP- 1	109.66	0.472	1707.33	0.9880
SEP- 2	78.47	19.41	1707.33	0.9841
RYEILD	364.03	0	1707.33	1.0000
CYCLONE	1204.40	0.660	1707.33	0.9963
COMBUSTOR	2002.70	374.66	1707.33	0.9960
GASIFIER	1874.3	717.02	1707.33	0.9961
COOLER- 1	58.51	0	1138.22	1.0000
HEATER- 2	78.47	16.85	1138.22	0.9514
COOLER-2	362.30	539.62	1138.22	0.6187
SEP- 3	362.30	539.62	1707.33	0.9904

Table 8. Results of exergoeconomic analysis of the study

COMPONENT	$C_{p,\,k}$	r_k%	$\dot{C}$ j	$\dot{C}_{D,k}\dot{E}_{p,k}$ fixed	$\dot{C}_{D,k}\dot{E}_{f,k}$ fixed
DRYER	0.812	0.0153	6602.20	2.056	1.0201
HEATER- 1	0.892	0.115	3065.99	2.589	2.887
SEP- 1	0.930	0.163	8855.71	20.158	23.434
SEP- 2	0.979	0.224	10052.79	27.598	33.773
RYEILD	0.000	-1.000	0	0	0
CYCLONE	0.811	0.0132	743666.63	6.400	6.488
COMBUSTOR	0.808	0.0101	192708.80	6.925	6.995
GASIFIER	0.807	0.00807	2825678.98	6.632	6.686
COOLER- 1	0.000	-1.000	0	0	0
HEATER- 2	3.922	3.902	13074.09	87.298	427.980
COOLER-2	4.233	4.291	976012.73	701.478	3711.698
SEP- 3	0.858	0.0729	110613.81	16.489	17.693

Table 9 shows comparative hydrogen production techniques and results from some reviewed works of literature. Results affirmed that an optimal peak operating efficiency can easily be achieved when considering the average unit cost of fuel $\dot{C}_{D,k}\dot{E}_{f,k}$ fixed with the product fixed as the main working fluid. However, this may not be beneficial for a component dryer, although its impact could be negligible since only one component is involved. Finally, the cycle performance curve drawing according to exergoeconomic multi-objective optimization results and its utilization are suggested.

Table 9. Comparative hydrogen production techniques and results from some reviewed works of literature

Reference	Work	Method (s)	Materials	Result (s)	Recommendation
Arzate et al [3]	Efficiency of an Au/TiO_2 photocatalyst for H_2 production and organic pollutant	Compound Parabolic Collector (CPC) at the Plataforma Solar de Almería (PSA)	Au/TiO2 photocatalyst, Wastewater as sacrificial agent	The energy efficiency of the process was 1.8%, and optimal catalyst loading was 0.2 g/L	Develop efficient photocatalysts, reuse catalysts, and test cheaper metals like Ni, and Cu.
Bing et al [4]	H_2 production from agricultural solid residue in Malaysia	ASPEN Plus to simulate the gasification process of palm oil biomass, Dual-fluidized bed reactor with NiO catalyst	ASPEN Plus software, palm oil biomass	The gasification process can produce H_2 with 95% purity.	Improving the efficiency of the gasification process and exploring the use of other catalysts
Boudries [5]	Techno-economic assessment of H_2 production in Algeria.	CPV-electrolysis system used for H_2 cost-effectiveness analysis	CPV-electrolysis system, PV-electrolysis.	A CPV-electrolysis system is an efficient and economical method of H_2.	Investigate CPV-electrolysis system parameters' effects and propose African-European collaboration to advance this technology.
Brynjarsdottir et al [7]	Effect of culture parameters on H_2 production	BM medium for culturing the strain GHL_{15}	Strain Thermo-anaerobacter GHL15	Thermoanaerobacter GHL15 yields 3.1 mol H_2/mol glucose at low H_2 pressure	Strain's sensitivity to initial substrate concentration and acetate accumulation
Jingwei et al [15]	H_2 production from biomass in supercritical water	Gasification in supercritical water (SCWG) and the use of concentrated solar energy	ASPEN Plus, glucose, corn meal, and wheat stalk, CSP power	Technical feasibility of the system and its advantages for H_2	Designing efficient reactors, continuous gasification of biomass with high dry matter
Hossain et al [12]	H_2 production from oil palm biomass by thermochemical process	Pyrolysis, gasification, and gasification in supercritical water.	Oil palm biomass,	Oil palm biomass is promising for H_2 due to high calorific value	Analysis of residual bio-char during H_2
Kalinci et al [13]	Life cycle assessment of H_2 production from biomass gasification systems	LCA to evaluate H_2 from biomass	Aspen plus, Life Cycle Assessment (LCA),	Downdraft Gasifier has lower fossil energy consumption and emissions compared to CFBG.	Combination of biomass and solar energy for H_2

Table 9 Continued.

Reference	Work	Method (s)	Materials	Result (s)	Recommendation
Kumar et al [24]	Comparative analysis of H_2 production from the thermochemical conversion of algal biomass	Techno-economic models, modeling, equipment sizing, and cost estimation	Algae biomass through thermal and supercritical water gasification	Supercritical water gasification is more cost-effective than thermal gasification	Improve algae biomass production, optimize processes, boost hydrogen yield, cut costs
Stefan et al [18]	H_2 production from biomass using a dual fluidized bed steam gasification system	IPSEpro to model the process, mass, and energy balance analysis	IPSEpro software, biomass as feedstock	61 MW of H_2 can be produced from 100 MW of wood chips and 6 MW of electricity	Improving the efficiency and cost-effectiveness of H_2 from biomass
Yaser et al [28]	Techno-economic analyses and life cycle assessments (LCA) of fluidized bed (FB) and entrained flow (EF)	Simulations and techno-economic analyses	Apen plus, fluidized bed (FB), and entrained flow (EF)	EF has 11% higher thermal efficiency than FB, and FB has a lower minimum H_2 selling price	Research needed to enhance efficiency and cut costs of biomass gasification
This study	Techno-economic analysis of a system for H_2 production from an empty banana fruit bunch	Aspen plus simulation, Biomass gasification	Empty banana fruit bunch, Aspen plus software	80.465 kg/h of H_2 from 2000 kg/h of EBFB at every instant of 39.92 km/h is feasible	Aligning temperature and pressure with CO_2 to boost H_2 production and reduce CO emissions

4. Conclusion

The research study was designed to simulate the production of hydrogen gas from an agricultural biomass residue, a quantified amount of empty banana fruit bunch, (EBFB) through biomass gasification for electricity generation. Aspen Plus version 11 was adopted for the simulation, the convectional exergy approach method for exergy analysis, and the Specific Cost method (SPECO) for exergoeconomic analyses. The following are the main study highlights:

- It has been observed that 80.465 kg/h of H_2 can be extracted from 2000 kg/h of empty banana fruit bunch at a constant mole flow rate of 39.92 km/h.
- The flow rates of H_2, O_2, N_2, and C in the combustor increase in a sinusoidal pattern at room temperature, while sulfur (S), in solid form, maintains a constant flow rate of 0.00 kg per hour. In the gasifier, the flow rates of H_2, CO_2, NH_3, and CH_4 decrease. In contrast, O_2, N_2, CO, and H_2O show an increase in flow content within the gasifier, while H_2S follows a linear trend.

- In the separator (SEP-3), the flow rate of H_2 increases from 3.525 kg/h to 3.62 kg/h, maintaining a linear trajectory. However, at a flow rate of 3.64 kg/h, H_2O decreases and settles at a linear rate of 3.52 kg/h. Consequently, both O_2 and CH_4 continue to follow a constant linear path.
- Carbon monoxide (CO) decreases and carbon dioxide (CO2) increases below 900 degrees Celsius. At temperatures of 1000 degrees Celsius and above, CO increases, which reduces CO2 emissions.
- The total exergy in, total exergy out, overall percentage exergy efficiency, and corresponding exergy destruction are 4534.77 kJ /kg, 3857.295 kJ /kg, 0.8506 %, and 677.475 kJ /kg respectively. The system exergy stream cost rate, component-related cost rate, component-related cost difference, and component exergoeconomic factor are: 407527.644 $/h, 1555.57 $/h, 0.5679 %, and 0.9089 %.

The author suggests that further research should be conducted under appropriate temperature and pressure conditions when working with CO_2. This approach aims to increase the production of H_2 while decreasing the emission of CO, thereby enhancing the overall CO_2 utilization. Additionally, it is essential to improve the exergy efficiency in specific components, including the cyclone, combustor, gasifier cooler-2, and SEP-3. Better performance can be achieved by adopting improved insulation and operational methods and reducing costs associated with investment and energy loss, specifically targeting low exergy destruction values.

Acknowledgment

I extend my sincere gratitude to the Federal University of Petroleum Resources for providing a conducive laboratory environment that greatly facilitated this research project.

Conflict of interest

There were no conflicts of interest during or after the course of this project. All research and findings were conducted independently and without any external influence.

Authors' Contributions

A. John: Conceptualization, Literature review, Methodology, Resources, Formal analysis, Writing - Original draft preparation (75 %)

J. Oyekale: Conceptualization, Supervision, Investigation (25 %).

All authors read and approved the final manuscript.

References

[1] AlZahrani, A. A., & Dincer, I. Integrated solar-based hydrogen extraction analysis. *International Journal of Hydrogen Energy*, *41*(19), 8042–8056. 2016. https://doi.org/10.1016/j.ijhydene.2015.12.103

[2] Amao, Y., Sakai, Y., &Takahara, S. Hydrogen Extraction from Solar via a cellulose biomass with an enzymatic system. *Chemical Research Intermediates*, *42*(11), 7753–7759. 2016. https://doi.org/10.1007/s11164-016-26602

[3] Arzate Salgado, S. Y., Ramírez Zamora, R. M., Zanella, R., Peral, J., Malato, S., & Maldonado, M. I. Photocatalytic Hydrogen Production. Foreign Energy Journal,*41*(28), 11933–11940. 2016. https://doi.org/10.1016/j.ijhydene.2016.05.039

[4] Bing, L. B., Chandrasekaran, P., Francis Xavier, V. D. C. S., Rajput, H. W., Ann, C. L., Mubarak, N. M., & Lau, S. Y. Hydrogen Extraction through Agricultural Solid Residue in Malaysia utilizing Aspen Plus Engineering Tool. Waste *and Biomass Valorization*, *11*(4), 1403–1419. 2020. https://doi.org/10.1007/s12649-018-0470-z

[5] Boudries, R. Techno-economic Assessment of Solar Hydrogen Production Using CPV-electrolysis Systems. *Energy Procedia*, *93*, 96–101. 2016. https://doi.org/10.1016/j.egypro.2016.07.155

[6] Boualati, Y., &Saouli, S. Experimental Study of Hydrogen Production Using Solar Energy in Ouargla (South East Algeria). *Journal of Solar Energy Engineering, Transactions of the ASME*, *140*(3). 2018. https://doi.org/10.1115/1.4039332

[7] Brynjarsdottir, H., Scully, S. M., &Orlygsson, J. Hydrogen Extraction through biohydrogen and lignocellulosic biomass. *International Journal of Hydrogen Energy*, *38*(34), 14467–14475. 2013. https://doi.org/10.1016/j.ijhydene.2013.09.005

[8] Cabezas, M. D., Franco, J. I., &Fasoli, H. J. Optimization of self-regulated hydrogen production from photovoltaic energy. *International Journal of Hydrogen Energy*, *45*(17), 10391–10397. 2020. https://doi.org/10.1016/j.ijhydene.2018.10.203

[9] Dimroth, F., Peharz, G., Wittstadt, U., Hacker, B., & Bett, A. W. (n.d.). *A PV concentrator using iii-v multi-junction solar cells for hydrogen.*

[10] Demirbas, A. Hydrogen through water gasification. *Part A: Recovery, Utilization and Environmental Effects*, *32*(14), 1342–1354. 2010. https://doi.org/10.1080/15567030802654038

[11] Ganeshan, I. S., Manikandan, V. V. S., Ram Sundhar, V., Sajiv, R., Shanthi, C., Kottayil, S. K., & Ramachandran, T.Regulated hydrogen production using a solar-powered electrolyzer. *International Journal of Hydrogen Energy*,*41(*24), 10322–10326. 2016. https://doi.org/10.1016/j.ijhydene.2015.05.048

[12] Hossain, M. A., Jewaratnam, J., & Ganesan, P. The prospect of hydrogen production through oil palm biomass – A review. In *International Journal of Hydrogen Energy* (Vol. 41, Issue 38, pp. 16637–16655. 2016. Elsevier Ltd. https://doi.org/10.1016/j.ijhydene.2016.07.104

[13] Kalinci, Y., Hepbasli, A., & Dincer, I. Hydrogen Life Cycle Assessment through Biomass. *International Journal of Hydrogen Energy*, *37*(19), 14026–14039. 2012. https://doi.org/10.1016/j.ijhydene.2012.06.015

[14] khanmohammadi, S., & Saadat-Targhi, M. Integrated system solar energy through waste food. *Energy*, *171*, 1066–1076. 2019. https://doi.org/10.1016/j.energy.2019.01.096

[15] Chen, J., Lu, Y., Guo, L., Zhang, X., & Xiao, P.Supercritical Hydrogen Extraction via Biomass.*International Journal of Hydrogen Energy*, *35*(13), 7134–7141. 2010. https://doi.org/10.1016/j.ijhydene.2010.02.023

[16] Marcantonio, V., de Falco, M., Capocelli, M., Bocci, E., Colantoni, A., &Villarini, M. Fluidized bed reactor with different separation systems. Foreign *Energy*, *44*(21), 10350–10360. 2019. https://doi.org/10.1016/j.ijhydene.2019.02.121

[17] Ma, Z., Zhang, S. P., Xie, D. Y., & Yan, Y. J.Novel hydrogen extraction via biomass energy. *International Journal of Hydrogen Energy*, *39*(3), 1274–1279. 2014. https://doi.org/10.1016/j.ijhydene.2013.10.146

[18] Müller, S., Stidl, M., Pröll, T., Rauch, R., &Hofbauer, H. Biomass hydrogen: Large-scale hydrogen production based on a dual fluidized bed steam gasification system. *Biorefinery*, *1*(1), 55–61. 2011. https://doi.org/10.1007/s13399-011-0004-4

[19] Xu, C., Chen, S., Soomro, A., Sun, Z., & Xiang, W.Hydrogen-rich syngas production through gasification of biomass. *Journal of the Energy Institute*, *91*(6), 805–816. 2018. https://doi.org/10.1016/j.joei.2017.10.014

[20] Zamfirescu, C., & Dincer, I. Assessment of a new integrated solar energy system for hydrogen production. *Solar Energy*, *107*, 700–713. 2014. https://doi.org/10.1016/j.solener.2014.05.036

[21] Zhang, L., Li, F., Sun, B., & Zhang, C. Intensified optimization design, and coupled power system. *Energies*, *12*(4). 2019. https://doi.org/10.3390/en12040687

[22] Samuel, O. D., Aigba, P. A., Tran, T. K., Fayaz, H., Pastore, C., Der, O., Erçetin, A., Enweremadu, C. C., & Mustafa, A. Comparison of the Techno-Economic and Environmental Assessment of Hydrodynamic Cavitation and Mechanical Stirring Reactors for the Production of Sustainable Hevea brasiliensis Ethyl Ester. *Sustainability*, *15*(23), 16287. 2023. https://doi.org/10.3390/su152316287

[23] Kitegi, M. S. P., Lare, Y., & Coulibaly, O. Potential for Green Hydrogen Production from Biomass, Solar, and Wind in Togo. *Smart Grid and Renewable Energy*, *13*(02), 17–27. 2022. https://doi.org/10.4236/sgre.2022.132002

[24] Kumar, M., Oyedun, A. O., & Kumar, A. A comparative analysis of hydrogen production from the thermochemical conversion of algal biomass. *International Journal of Hydrogen Energy*, *44*(21), 10384–10397. 2019. https://doi.org/10.1016/j.ijhydene.2019.02.220

[25] Li, D., Ishikawa, C., Koike, M., Wang, L., Nakagawa, Y., &Tomishige, K. Renewable Hydrogen-supported Co catalysts. *International Journal of Hydrogen Energy*, *38*(9),3572–3581. 2013. https://doi.org/10.1016/j.ijhydene.2013.01.057

[26] Liu, Q., Bai, Z., Wang, X., Lei, J., &Jin, H. Investigation of thermodynamic performances for two solar-biomass hybrid combined cycle power generation systems. *Energy Conversion and Management*, *122*, 252–262. 2016. https://doi.org/10.1016/j.enconman.2016.05.080

[27] Sakr, I. M., Abdelsalam, A. M., & El-Askary, W. A. Electrode demerit on hydrogen extraction via solar. *Energy*, *140*, 625–632. 2017. https://doi.org/10.1016/j.energy.2017.09.019

[28] Salkuyeh, Y. K., Saville, B. A., & MacLean, H. L.Techno-economic analysis and life cycle assessment hydrogen through biomass. *International Journal of Hydrogen Energy*, *43*(20), 9514–9528. 2018. https://doi.org/10.1016/j.ijhydene.2018.04.024